

# Biotrickling Filtration for the Reduction of N<sub>2</sub>O Emitted during Wastewater Treatment: Results from a Long-Term In Situ Pilot-Scale Testing

Heejoon Han, Daehyun D. Kim, Min Joon Song, Taeho Yun, Hyun Yoon, Hong Woon Lee, Young Mo Kim, Michele Laurenzi, and Sukhwan Yoon\*



Cite This: *Environ. Sci. Technol.* 2023, 57, 3883–3892



Read Online

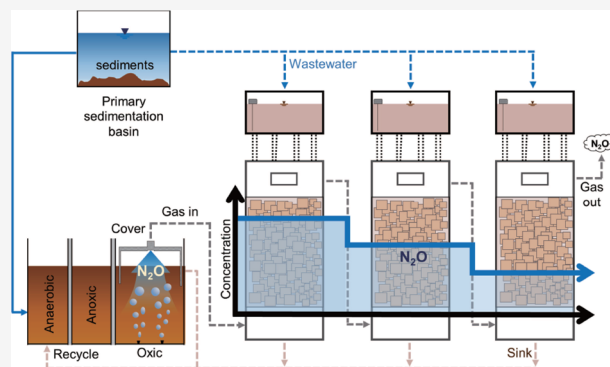
ACCESS |

Metrics & More

Article Recommendations

Supporting Information

**ABSTRACT:** Wastewater treatment plants (WWTPs) are a major source of N<sub>2</sub>O, a potent greenhouse gas with 300 times higher global warming potential than CO<sub>2</sub>. Several approaches have been proposed for mitigation of N<sub>2</sub>O emissions from WWTPs and have shown promising yet only site-specific results. Here, self-sustaining biotrickling filtration, an end-of-the-pipe treatment technology, was tested in situ at a full-scale WWTP under realistic operational conditions. Temporally varying untreated wastewater was used as trickling medium, and no temperature control was applied. The off-gas from the covered WWTP aerated section was conveyed through the pilot-scale reactor, and an average removal efficiency of 57.9 ± 29.1% was achieved during 165 days of operation despite the generally low and largely fluctuating influent N<sub>2</sub>O concentrations (ranging between 4.8 and 96.4 ppmv). For the following 60-day period, the continuously operated reactor system removed 43.0 ± 21.2% of the periodically augmented N<sub>2</sub>O, exhibiting elimination capacities as high as 5.25 g N<sub>2</sub>O m<sup>-3</sup>·h<sup>-1</sup>. Additionally, the bench-scale experiments performed abreast corroborated the resilience of the system to short-term N<sub>2</sub>O starvations. Our results corroborate the feasibility of biotrickling filtration for mitigating N<sub>2</sub>O emitted from WWTPs and demonstrate its robustness toward suboptimal field operating conditions and N<sub>2</sub>O starvation, as also supported by analyses of the microbial compositions and *nosZ* gene profiles.



**KEYWORDS:** nitrous oxide, biotrickling filtration, activated sludge, metagenome, nitrous oxide reductase, in situ pilot test

## INTRODUCTION

Nitrogen, along with organic carbon and phosphorous, is the primary target of municipal sewage treatment.<sup>1,2</sup> In a typical WWTP implementing biological nitrogen removal (BNR), NH<sub>4</sub><sup>+</sup> is aerobically oxidized to NO<sub>3</sub><sup>-</sup>, and internally recycled NO<sub>3</sub><sup>-</sup> is reduced to N<sub>2</sub>. These microbial reactions contribute to the production and emission of N<sub>2</sub>O, a greenhouse gas with a global warming potential ~300 times greater than CO<sub>2</sub>.<sup>3–7</sup> Recent studies estimate that N<sub>2</sub>O emissions may account for >50% of wastewater treatment plants' (WWTPs') carbon footprints, calling for the urgent development of mitigation strategies.<sup>8,9</sup>

Nitrification and denitrification are known to be the microbial pathways responsible for most of the N<sub>2</sub>O produced and emitted during BNR processes.<sup>3,6,8</sup> Previous studies have attributed N<sub>2</sub>O production to incomplete heterotrophic denitrification, abiotic turnover of hydroxylamine produced from ammonia oxidation, and nitrifier denitrification.<sup>6,9</sup> The relative contributions of these sources vary across WWTPs and temporally within a given WWTP, and thus, whether anoxic

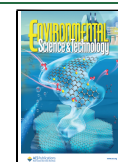
(denitrification) or aerobic (nitrification) processes are the major culprits of N<sub>2</sub>O emissions from WWTPs remains ambivalent.<sup>8,10</sup> Another confounding common observation reported from recent long-term in situ N<sub>2</sub>O monitoring campaigns is the large temporal emissions variability that has eluded parametrization and/or modeling efforts.<sup>8,11,12</sup> In a recent monitoring campaign at a full-scale A2O (anaerobic–anoxic–oxic)-type WWTP in South Korea, the aerated-segment N<sub>2</sub>O fluxes measured in two contiguous months differed by as much as 10-fold (17.5 g N<sub>2</sub>O–N m<sup>-2</sup> d<sup>-1</sup> in August vs 1.7 g N<sub>2</sub>O–N m<sup>-2</sup> d<sup>-1</sup> in September).<sup>8</sup> Similar inexplicable variabilities were observed in the dissolved N<sub>2</sub>O

Received: November 23, 2022

Revised: February 13, 2023

Accepted: February 13, 2023

Published: February 21, 2023



concentrations monitored at a carousel-type BNR reactor in Denmark over a 2-year period.<sup>11</sup>

Earlier mitigation efforts focused mostly on reducing N<sub>2</sub>O production via modulation of WWTP operation conditions.<sup>13–15</sup> Several operating parameters, including dissolved oxygen (DO) concentration and chemical oxygen demand-to-nitrogen ratio (COD/N), have been suggested to affect N<sub>2</sub>O emissions from nitrification and denitrification, and N<sub>2</sub>O emission mitigation efforts via optimization of these parameters have yielded promising results at limited temporal and spatial scales.<sup>16,17</sup> However, considering the aforementioned lack of consistency in N<sub>2</sub>O generation and emission mechanisms, and the dynamics recently witnessed within and across WWTPs, the general efficacy of such approaches remains questionable at best.

More recently, end-of-the-pipe N<sub>2</sub>O elimination technologies are gaining attention as alternative N<sub>2</sub>O emission control strategies for WWTPs.<sup>18–20</sup> Resorting to biological processes is often considered the most appropriate solution for the removal of trace pollutants occurring at micro- or nanomolar concentrations in soil and aquatic environments, as microbial metabolisms are diverse and resilient, and their engineering implementation generally requires relatively little input of chemicals and energy.<sup>21–23</sup> Microorganisms capable of reducing N<sub>2</sub>O to N<sub>2</sub> are no exception: their phylogenetical and phenotypical diversity enables effective N<sub>2</sub>O reduction at a broad range of concentrations and confers robustness to communities' aggregate N<sub>2</sub>O-reducing capability.<sup>24–26</sup> Recent investigations have revealed that groups of N<sub>2</sub>O-reducing microorganisms possessing clade II *nosZ*, namely *Dechloromonas* spp. and *Azospira* spp., exhibit remarkably high affinity toward N<sub>2</sub>O and, therefore, would effectively consume N<sub>2</sub>O at the range of concentrations detectable in WWTP off-gases.<sup>26–28</sup> Further, the omnipresence and abundance of these putative efficient N<sub>2</sub>O consumers in activated sludge microbiomes render these organisms as promising biocatalysts for WWTP-related engineered systems.<sup>29,30</sup>

A central hurdle in developing biological N<sub>2</sub>O emission mitigation technologies for WWTP has been the inactivation of *NosZ*-mediated N<sub>2</sub>O reduction under oxic conditions.<sup>31–33</sup> Earlier, Yoon et al. devised a biotrickling filtration system that circumvented this challenge and achieved substantial N<sub>2</sub>O removal from fully oxic gases by exploiting the different degree to which O<sub>2</sub> and N<sub>2</sub>O diffuse into wet films, demonstrating the technical feasibility of the approach.<sup>19,20</sup> However, many factors that may affect long-term in situ performance of the system awaited to be assessed toward full-scale implementation of the technology. The previously reported laboratory systems were fed with synthetic wastewater, and the impacts of diurnal and seasonal temperature fluctuations and varying influent N<sub>2</sub>O concentrations on the system performance have not yet been examined. Here, an in situ long-term test was performed using a pilot-scale biotrickling filtration system integrated into a full-scale WWTP to examine the performance of the reactor under the stressors unaccounted for in the laboratory experiments. Furthermore, the effect of intermittent short-term N<sub>2</sub>O starvations to the biofiltration performance was examined with bench-scale reactor operated in situ, which enabled a tighter control of the inlet N<sub>2</sub>O concentration.

## MATERIALS AND METHODS

**Site Information.** All experiments were performed at a typical full-scale A2O (anaerobic–anoxic–oxic) WWTP

located in Gapyeong, Korea (37.816491° N, 127.520316° E). The WWTP consists of four identical trains, each treating 2850 m<sup>3</sup> d<sup>-1</sup> of wastewater at a hydraulic retention time of 11.0 h and a solid retention time of 10.2 d (Figure S1). The minimum and maximum mean monthly average air temperatures recorded during the period of study (September 2018 to November 2019) were  $-7.8 \pm 5.0$  and  $31.2 \pm 2.9$  °C, respectively. The region received highly variable precipitation, with the monthly net precipitation ranging between 15.9 mm (November, 2018) and 252.2 mm (July, 2019) during the period of study (Table S1).

**Installation and Operation of the In Situ Pilot-Scale N<sub>2</sub>O-Removal Biotrickling Filtration System.** A pilot-scale N<sub>2</sub>O biotrickling filtration system was constructed at the Daega Powder Systems Co. factory (Seoul, South Korea) and transported to Gapyeong WWTP (Figure S2). The pilot-scale system consisted of three rectangular filter columns with 1300 L empty bed volume, of which 400 L was packed with 4 × 4 × 4 (cm) polyurethane foams. Each filter column was fitted with an open 220 L water storage tank placed on top. Each tank was equipped with a water level sensor, which automatically switched on a 0.95 kW pump to refill the tank with wastewater drawn from the primary sedimentation basin when the water surface level dropped below the preset threshold. The trickling rate was approximately 2.4 L min<sup>-1</sup> column<sup>-1</sup>. This design emulates the conceptual design where, elevation-wise, the filter columns are to be positioned between a primary sedimentation basin and an activated sludge tank such that the columns are supplied with gravitationally fed wastewater.<sup>19</sup> The oxic segment of the activated sludge tank, aerated at a nominal flux of 1.95 L m<sup>-2</sup> s<sup>-1</sup>, was partially covered with a floating 5 m × 6 m polycarbonate cover with a submerged depth of 0.3 m. An air duct with an inner diameter of 11 cm connected the covered headspace to the biotrickling filtration system. The gas flowrate into the biotrickling filters was controlled with an air damper and, thus, was decoupled from the aeration rate of the activated sludge tank. Gas samples for N<sub>2</sub>O concentration measurements were collected from the sampling ports installed at the inlet of each filter column and the gas outlet from the system. As the temperature of the gas effluent from the reactor was not statistically different from the ambient air temperature ( $p > 0.05$ ), only the ambient air temperature is presented (Figure S3).

The start-up procedure for the initial testing of the pilot-scale biotrickling filtration system began on October 31, 2018. Initially, N<sub>2</sub>O-reducing biofilms were enriched in the biotrickling filters via 168 h of anoxic incubation with N<sub>2</sub> gas containing ~100 ppmv N<sub>2</sub>O (Gyeongwon Co., Wonju, Korea) passing through each filter column at a volumetric flowrate of 300 L h<sup>-1</sup>. After the start-up procedure, the gas tanks were detached from the biotrickling filters, and the air duct leading from the activated sludge tank cover was connected to the system inlet, and the three filter columns were connected in a serial manner (day 0 in Figure S4). The initial testing of the pilot-scale biofiltration system ended after 29 days of operation. The long-term system operation and monitoring began after the winter hiatus with an identical start-up procedure and treated unaltered waste gas from the activated sludge tank until day 165 (day 0 being March 4).

Without discontinuation or disruption of reactor operation, the performance of the reactor system was then examined with N<sub>2</sub>O-augmented gas streams over four short periods (days 175–184, 203–207, 229–235, and 253–256). During these

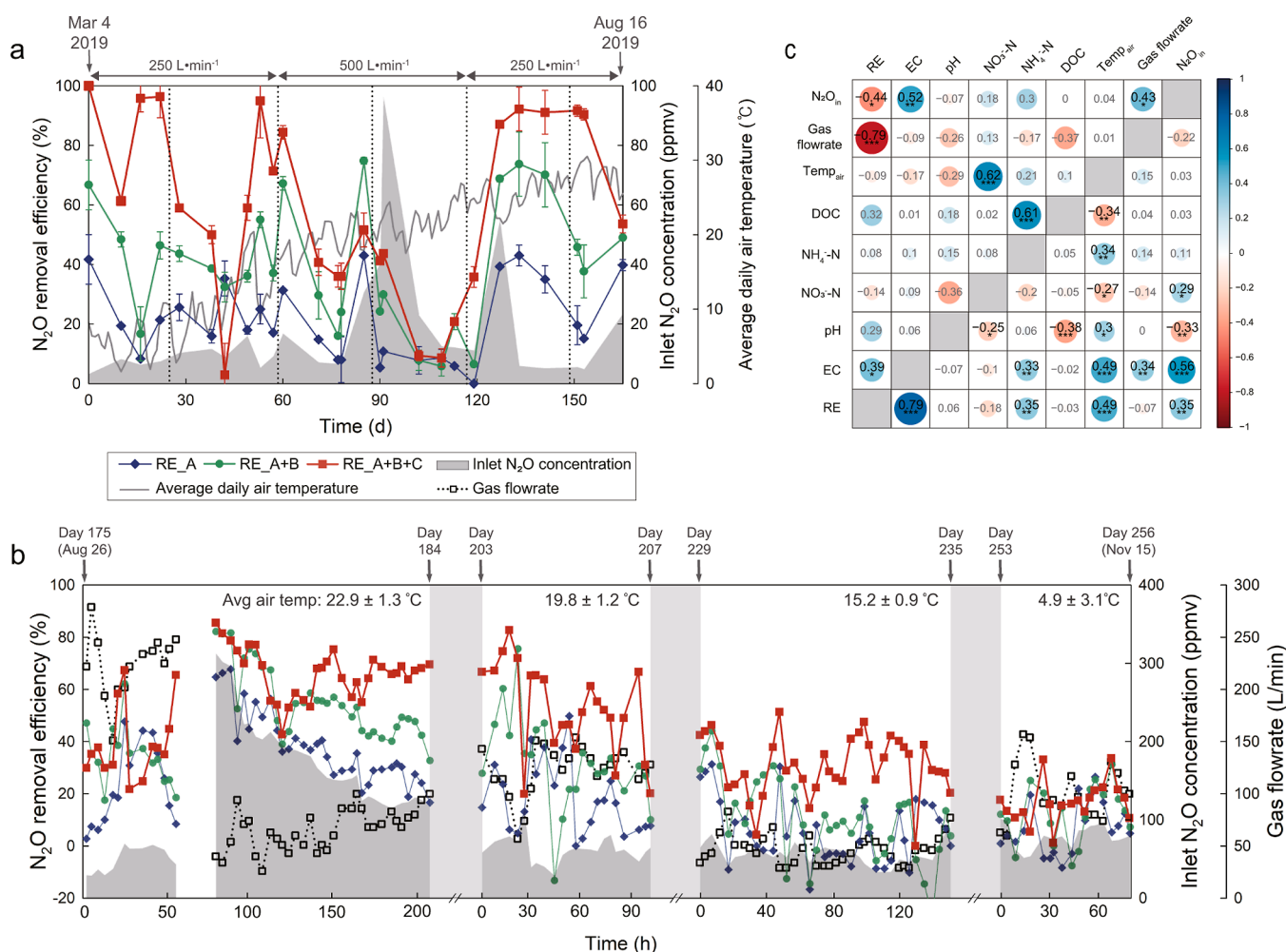


**Figure 1.** Performance of the pilot-scale biotrickling filtration system through the continuous operation from March to November 2019 conducted in two phases, i.e., (a) day 0–165 without N<sub>2</sub>O augmentation and (b) day 175–256 with periodic N<sub>2</sub>O augmentation. The cumulative N<sub>2</sub>O removal efficiencies after treatment in the filter columns A (◆), B (●), and C (■) are presented. The measured N<sub>2</sub>O concentration at the system inlet was presented in dark gray shading. Additionally, the average daily ambient air temperature (gray line) is shown in the panel (a), and the gas flowrate (□) is presented in the panel (b). The legend applies to both panels (a,b). (c) The graphical correlation matrices, constructed with the data collected from the pilot plant operation (left: day 0–165; right: day 175–256), illustrate the significance and the strengths of correlations between the operating parameters and conditions and the N<sub>2</sub>O-removal performance (RE and EC) of the system. The size and color of the circle indicate the sign and the magnitude of the correlation, respectively, and the number of the asterisk mark(s) denotes the strength of the statistical significance (\**p* < 0.05, \*\**p* < 0.01, \*\*\**p* < 0.001).

periods, the main gas stream was augmented with a stream of 20:80 N<sub>2</sub>O/air mixed gas with negligible flowrates (<0.1 L min<sup>-1</sup>), such that the total gas flowrate and the chemical composition of the waste gas were unaffected while the N<sub>2</sub>O concentration was augmented to 28–312 ppmv. During the interim periods between the N<sub>2</sub>O augmentation experiments, the reactor system was continuously operated without N<sub>2</sub>O augmentation. The originally planned continuation of the long-term operation through the year 2020 had to be cancelled due to the COVID-19 situation in South Korea.

**In Situ Experiments with the Bench-Scale Biotrickling Filtration System.** A bench-scale biotrickling filtration system, previously used for the laboratory tests, was operated alongside the pilot-scale system (Figure 1) to independently examine the response of the N<sub>2</sub>O removal performance to short-term N<sub>2</sub>O starvations.<sup>19,20</sup> Three cylindrical filter columns with 1000 mm height and 160 mm inner diameter were packed with polyurethane foams cut into 2 × 2 × 2 cm cubes to a packed bed volume of 16.1 L. Wastewater pumped

from the primary sedimentation basin was passed through each filter column at 89 mL min<sup>-1</sup>. N<sub>2</sub>O-reducing biofilms were established by the start-up operation, during which N<sub>2</sub> gas containing ~100 ppmv N<sub>2</sub>O was passed through each filter column in a parallel manner at a flowrate of 600 mL·min<sup>-1</sup>. After 168 h, the gas source was changed to air containing ~100 ppmv N<sub>2</sub>O (Gyeongwon Co.), and the system setup was changed to a serial configuration. After operating with air carrying 100 ppmv N<sub>2</sub>O as the influent gas for 150 days, the influent N<sub>2</sub>O concentration was intentionally varied, using air containing four different concentrations of N<sub>2</sub>O (100, 50, 20, and 0 ppmv). The gas canisters were switched every 40 h to lower the influent N<sub>2</sub>O concentration in a stepwise manner and then gradually raise it back after 40 h of starvation. Gas samples for determination of N<sub>2</sub>O concentration were collected every 3–4 h. The experiments were repeated three times, once each month from August to October. During the intervening periods between the experiments, the reactor system was operated with air containing 100 ppmv N<sub>2</sub>O. The



gas flowrate was maintained constant at 600 mL·min<sup>-1</sup> throughout the experiment regardless of the N<sub>2</sub>O concentration.

**Sample Collection and Analytical Procedures.** The gas samples for N<sub>2</sub>O concentration measurements were collected using Tedlar gas sampling bags (pilot) or disposable syringes (bench). Duplicate gas samples were collected with a 120 min (pilot) or 30 min interval (bench). N<sub>2</sub>O concentrations were measured using an HP6890 series gas chromatograph equipped with an electron capture detector (Agilent, Palo Alto, CA).<sup>20</sup>

The removal efficiency (RE) and elimination capacity (EC) were calculated based on the measured N<sub>2</sub>O concentrations (eqs 1 and 2).

$$\text{RE (\%)} = \frac{C_{\text{in}} - C_{\text{out}}}{C_{\text{in}}} \times 100 \quad (1)$$

$$\text{EC} = \frac{C_{\text{in}} - C_{\text{out}}}{V} \times Q_{\text{gas}} \quad (2)$$

where  $C_{\text{in}}$  and  $C_{\text{out}}$  are the system inlet and outlet N<sub>2</sub>O concentrations (ppmv), respectively,  $V$  is the bed volume (m<sup>3</sup>), and  $Q_{\text{gas}}$  is the instantaneous gas flowrate (m<sup>3</sup> h<sup>-1</sup>). The gas flowrate of the pilot-scale system was measured at the system inlet and outlet with an Omniport 30 device (E + E Elektronik GmbH, Engerwitzdorf, Austria).

The chemical properties of the wastewater in the primary sedimentation basin were also monitored. Wastewater was grab-sampled from the tank, and the pH and water temperature were immediately measured. After a brief settling, the supernatant was filtered through a 0.45 μm syringe filter (Jet Bio-Filtration Co., Guangzhou, China), and the filtrate was immediately frozen in a -20 °C freezer. The concentrations of NO<sub>3</sub><sup>-</sup>, NO<sub>2</sub><sup>-</sup>, and NH<sub>4</sub><sup>+</sup> were measured using colorimetric methods as previously described.<sup>34,35</sup> The dissolved organic carbon (DOC) concentration was measured with a TOC-L TOC analyzer (Shimadzu, Kyoto, Japan).

The polyurethane foam elements were collected from the middle of each column bed for microbial analyses of the biofilms. The biofilm samples were collected from the pilot-scale filter columns each month from August to November 2019, and from the bench-scale filter columns each month from July to October 2019. The polyurethane foams were placed in 500 mL glass bottles (pilot) or sterilized 50 mL conical tubes (bench) and immediately frozen and stored at -20 °C. For the extraction of DNA from the biofilms, the polyurethane cubes were thawed on ice in a new 50 mL Falcon tube, to which 30 mL sterilized double-distilled water was added. The tube was vortexed for 5 min and sonicated for 10 min, and DNA was extracted from 2 mL of the cell suspension using the DNeasy PowerSoil DNA Isolation Kit (QIAGEN Hilden, Germany).

**Bioinformatics Analyses.** For analyses of the microbial compositions of the biofilms, the V6–V8 region was amplified with the 926F (5'-AACTYAAAKGAATTGRCGG-3') and 1392R (5'-ACGGGCGGTGTGTRC-3') primer set and sequenced at Macrogen Inc. (Seoul, Korea) using the MiSeq sequencing platform (Illumina, San Diego, CA). The quality-trimmed and merged reads were processed using the QIIME2 v2020.8 pipeline, and the amplicon sequence variants (ASV) were assigned taxonomic classification using the naïve Bayes scikit-learn classifier pre-trained with SILVA SSU Ref NR 99 database release 138.<sup>36</sup>

Select biofilm samples were subjected to shotgun metagenome analysis for identification, taxonomic classification, and relative quantification of *nosZ* genes. Shotgun metagenomes were sequenced as paired-end reads (2 × 150 bp) on an Illumina HiSeq 4000 platform at Macrogen Inc. with a targeted throughput of 5 Gb. The quality-trimmed reads acquired from the four sequenced metagenomes were combined and assembled *de novo* using metaSPAdes v3.14.0.<sup>37</sup> Gene-coding sequences were predicted and translated *in silico* using Prodigal v2.6.3 and annotated using DIAMOND blastp v0.9.29 against NCBI's nr database (accessed September 1, 2020) with the *e*-value cutoff set to 1E-10 and the minimum identity and query coverage set to 30 and 70%, respectively.<sup>38,39</sup> The quality-trimmed raw reads from each sample were mapped separately onto the *nosZ*-containing contigs using the Bowtie2 v2.3.5.1 (default parameters), and their coverages (reads per kilobase of contig) were normalized by the tallied coverage of all *rpoB*-containing contigs from the same sample.<sup>40–42</sup> The closest full-length blastp hits (limited to those with *e*-value < 1E-20 and identity > 70%) to the unique full and partial metagenomic *NosZ* sequences were downloaded from the NCBI nr protein database, and these sequences were organized into clusters with a 75% amino acid similarity threshold using cd-hit v4.6.<sup>43</sup> The metagenomic sequences were distributed into these clusters according to the affiliation of their best blastp hits. The putative *NosZ* sequences not meeting the *e*-value and identity thresholds or not belonging to any of the 19 major clusters were discarded, as none of these sequences was found in substantial abundance in any of the metagenomes (<0.0005 *nosZ/rpoB*). All raw amplicon and metagenomic sequence data were deposited in the NCBI SRA database (accession number: PRJNA842158).

**Statistical Analyses.** Statistical analyses were performed with the R statistical software package (version 4.0.2) via the R Studio (v. 1.3.959) interface.<sup>44</sup> Statistical significance of a pairwise comparison was evaluated using Tukey's honestly significant difference *post-hoc* tests or Wilcoxon rank-sum tests. Kruskal–Wallis tests were used for statistical evaluation of comparison among  $n \geq 3$  samples. The significance threshold was set to a *p*-value of 0.05. The pairwise correlations between the parameters were analysed via Spearman's rank correlation analyses.

## RESULTS

**Physicochemical Characterization of Wastewater Supplied to the Filter Columns.** The characteristics of the wastewater in the primary sedimentation basin, supplied to the filter columns as the trickled medium, were temporally variable (Table S1). The highest and the lowest monthly average water temperatures in the primary sedimentation basin were 16.1 ± 0.1 °C (Dec 2018) and 22.4 ± 0.5 °C (August 2019), respectively. The pH values fluctuated between 6.0 and 7.9 without any distinct trend. The monthly average DOC concentrations ranged between 15.6 ± 0.7 (October 2018) and 40.5 ± 10.2 mg/L (March 2019). Dissolved nitrogen consisted mostly of NH<sub>4</sub><sup>+</sup>, with the monthly average NH<sub>4</sub><sup>+</sup>-N concentrations varying between 11.9 ± 2.3 mg/L (September 2018) and 26.2 ± 1.9 mg/L (July 2019).

**Long-Term Performance Consistency of the Pilot-Scale System.** The data collected from the pilot-scale operation showed that, from a technical perspective, consistent mitigation of N<sub>2</sub>O emission from a BNR system is feasible using biotrickling filtration under realistic *in situ* operating

conditions (Figure 1). After the brief initial 30 day test run in 2018 (the result presented in Figure S4), the pilot-scale system was continuously operated for 256 days (day 0 being March 4, 2019) in two phases: day 0–165 without gas amendment and day 175–256 with periodic N<sub>2</sub>O augmentation. Despite the largely fluctuating and unanticipatedly low influent N<sub>2</sub>O concentrations, the pilot plant removed  $57.9 \pm 29.1\%$  of  $16.6 \pm 19.5$  ppmv N<sub>2</sub>O in the waste-gas stream introduced between day 0 and 165, averaging an EC of  $0.96 \pm 1.34$  g N<sub>2</sub>O m<sup>-3</sup>·h<sup>-1</sup>. Although short periods of diminished RE were observed, e.g., between day 102 and 109, the system performance recovered spontaneously.

Starting from day 175, the operation of the pilot plant was continued with periodical N<sub>2</sub>O supplementation, exhibiting a consistent removal of >50 ppmv N<sub>2</sub>O until the system started to be adversely affected by the wintry weather (Figure 1b). The biotrickling filtration system removed  $47.6 \pm 19.4\%$  of N<sub>2</sub>O in the gas stream during the three N<sub>2</sub>O augmentation experiments performed between day 175 and 235. The performance during these experiments, in terms of RE and EC, was comparable with those observed between days 85 and 91 and on day 127 ( $55.9 \pm 18.4\%$  RE and  $3.63 \pm 1.56$  g N<sub>2</sub>O m<sup>-3</sup>·h<sup>-1</sup> EC) when the N<sub>2</sub>O concentration in the waste gas peaked above 30 ppmv. The observations from these N<sub>2</sub>O augmentation experiments suggested that the biotrickling filtration system would exhibit a larger N<sub>2</sub>O EC if installed at facilities with consistently higher N<sub>2</sub>O emissions, as also supported by the significant positive correlations between the influent N<sub>2</sub>O concentration and EC ( $p < 0.01$  for both phases; Spearman's rank correlation test; Figure 1c). The performance of the system was clearly diminished in the experiment performed between days 253 and 256, as the average daily air temperature dropped to  $4.9 \pm 3.1$  °C. During this period, occasional production of N<sub>2</sub>O was observed in individual filter columns; however, net negative N<sub>2</sub>O removal was prevented, thanks to the serial configuration of the system (the red curve in Figure 1b).

Throughout the two phases of the pilot-plant operation, the biotrickling filtration system exhibited performance robustness toward widely varying operating conditions (Figure 1c). No significant correlation between either RE or EC and any of the examined physicochemical parameters (i.e., the daily average air temperature, DOC, NH<sub>4</sub><sup>+</sup>-N, NO<sub>3</sub><sup>-</sup>-N, and pH) was observed during the phase without gas amendment. In the analysis performed with the data collected from the N<sub>2</sub>O-augmentation experiments, the daily average air temperature exhibited strong positive correlations with both RE and EC ( $p < 0.001$ ), statistically supporting the observed vulnerability of the system to wintry weather. No chemical parameter apart from NH<sub>4</sub><sup>+</sup>-N concentration correlated significantly with either RE or EC in this dataset ( $p > 0.05$ ).

**Resilience to Short-Term N<sub>2</sub>O Starvations (Bench-Scale).** The bench-scale experiment was designed to examine the response of the filter system to intermittent N<sub>2</sub>O starvations, events that are expected to frequently occur during full-scale operations but could not be effectively examined with the pilot plant (Figure 2). The bench-scale reactor had been operated with consistent RE ( $51.6 \pm 15.4\%$ ; Figure S5) for 150 days before a series of short-term experiments simulating intermittent N<sub>2</sub>O starvations were performed. A gradual decrease in the inlet N<sub>2</sub>O concentration resulted in significantly reduced RE ( $p < 0.05$ ) (Figure 2a,b). During the experiment performed in August, RE decreased to  $22.6 \pm$

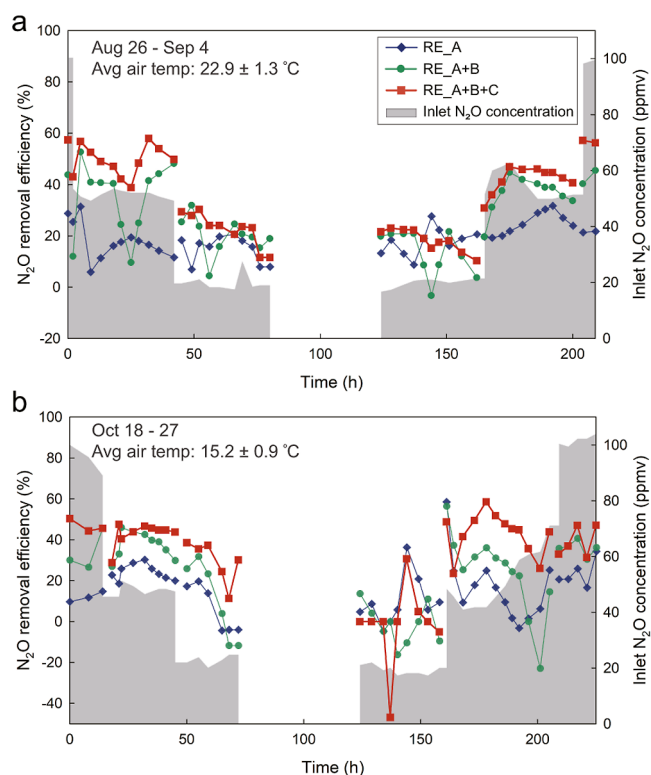


**Figure 2.** Performance of the bench-scale biotrickling filtration system during the short-term experiments performed with a 40 h N<sub>2</sub>O starvation in (a) August and (b) October 2019. The cumulative N<sub>2</sub>O removal efficiencies after treatment in the filter columns A (◆), B (●), and C (■) are presented. The shaded areas represent the measured inlet N<sub>2</sub>O concentrations. The result from the replicate short-term experiment performed in September 2019 is shown in Figure S6.

6.2% as the influent N<sub>2</sub>O concentration was lowered from 50 to 20 ppmv. Apparently, 40 h of N<sub>2</sub>O starvation did not significantly affect the performance of the biotrickling filtration system, as RE measured before and after the starvation period were not significantly different at either influent N<sub>2</sub>O concentration ( $p > 0.05$ ). The replicate experiment performed between September 23 and October 2 yielded statistically indistinguishable RE at each stage (Figure S6). Interestingly, in the experiment performed when the daily average air temperature decreased to  $15.2 \pm 0.9$  °C (Oct 18–27), the capability to remove N<sub>2</sub>O did not immediately recover when the influent N<sub>2</sub>O concentration was increased back to 20 ppmv after starvation ( $-1.8 \pm 18.7$  vs  $29.6 \pm 9.5\%$  before starvation;  $p < 0.05$ ), and the performance at 20 ppmv N<sub>2</sub>O concentration was unstable. Nevertheless, the performance was fully recovered to the level on par to that measured before starvation when the inlet N<sub>2</sub>O concentration was increased back to 50 ppmv ( $40.7 \pm 7.5\%$  RE;  $p > 0.05$ ). These observations suggested that not only removal performance but also the resilience of the system to short-term N<sub>2</sub>O starvations may be affected by the wintry weather condition, especially when the baseline N<sub>2</sub>O concentration is low, although the process otherwise proved to be only marginally impacted by short periods of N<sub>2</sub>O absence.

**Biofilm Microbial Community Composition and *nosZ* Profiles.** The microbial compositions of the biofilms showed a relative robustness toward both fluctuating bulk-gas N<sub>2</sub>O concentrations and temporally varying wastewater character-

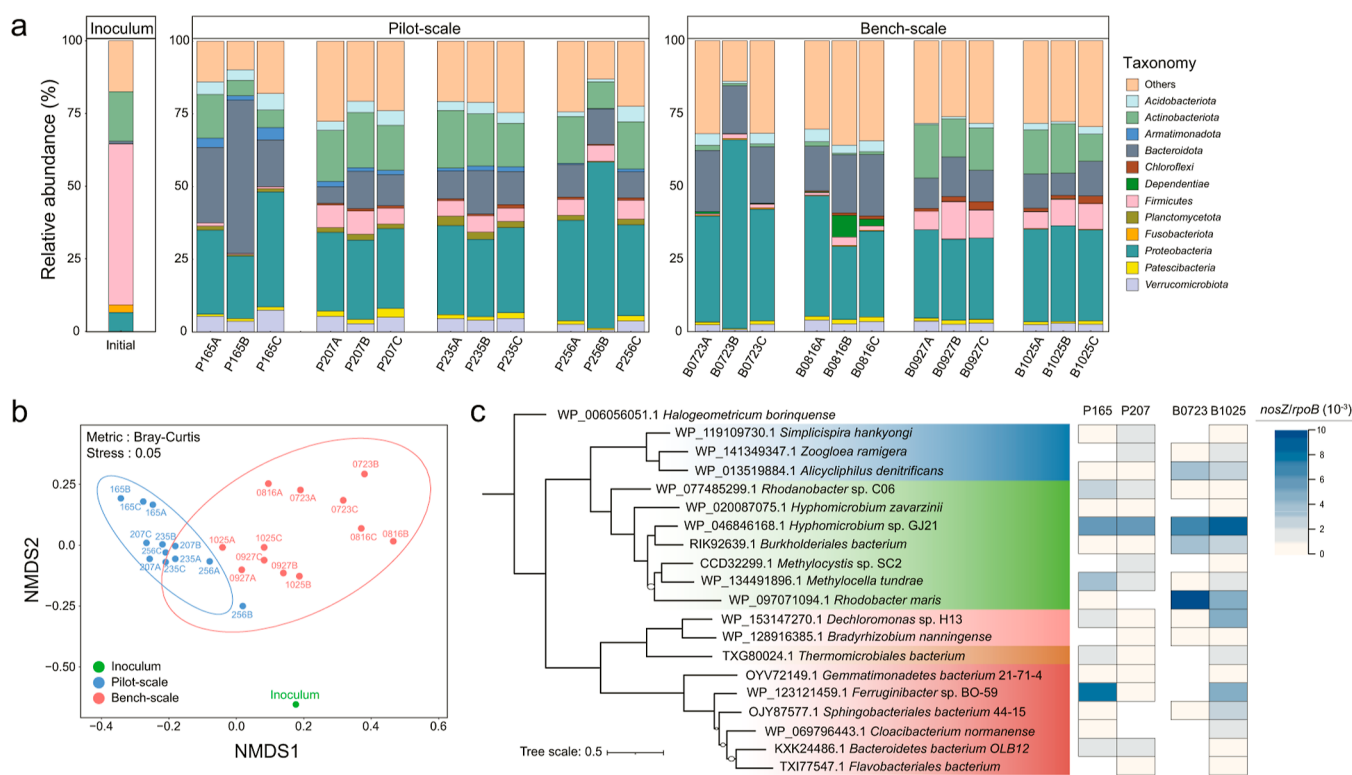


**Figure 3.** Biofilm microbial compositions and *nosZ* profiles. (a) Time-series microbial community analyses of the biofilms sampled from the pilot-scale filter columns A, B, and C (left: between day 165 and 256) and the bench-scale filter columns A, B, and C (right: between July 23 and October 25, 2019). The ASVs (complete data presented in Table S4) from 16S rRNA gene amplicon sequencing have been organized to phylum-level taxa. The numbers in the *x*-axis labels indicate the time of sampling (the day number and the date for the pilot-scale data and the bench-scale data, respectively). (b) The beta diversity of the biofilm communities visualized in a Bray–Curtis non-metric multidimensional scaling (NMDS) plot. The numbers indicate the time of sampling. (c) Maximum-likelihood phylogenetic tree constructed for the 19 clusters of metagenomic *nosZ* sequences. Each cluster was represented by the best BLASTP hit of the NosZ sequence translated *in silico* from the most abundant metagenomic *nosZ* within the cluster. Bifurcations with <50% bootstrap support are indicated with circles. The archaeal *nosZ* of *Halogeometricum borinquense*, downloaded from the NCBI database, was added as the outgroup. The abundances of each *nosZ* cluster, as normalized by the abundances of the single-copy housekeeping gene *rpoB* in the respective metagenomes, are presented in the heatmap on the right.

istics, while also featuring modest seasonal transitions from summer to fall (Figure 3a, Tables S2, S3 and S4). The pilot- and bench-scale reactor biofilms were largely similar in their compositions, as shown with the non-metric multidimensional scaling (NMDS) analysis (Figure 3a,b). The periodic N<sub>2</sub>O augmentation to the pilot plant had a limited impact on the overall microbial composition, i.e., samples collected before (day 165) and during N<sub>2</sub>O augmentation (day 207–256) showed largely similar compositions. Similarly, short-term starvation did not substantially affect the bench-scale biofilms.

The most abundant taxa in the biofilms, at the phylum level, were *Actinobacteria* ( $14.4 \pm 4.7$  and  $7.8 \pm 7.1\%$  in the pilot-scale and bench-scale reactor biofilms, respectively), *Bacteroidota* ( $16.0 \pm 12.0$  and  $15.0 \pm 4.4\%$ ), *Firmicutes* ( $4.7 \pm 2.5$  and  $5.1 \pm 4.0\%$ ), and *Proteobacteria* ( $31.8 \pm 8.8$  and  $34.9 \pm 10.1\%$ ). Apart from *Bacteroidota*, these phyla were also the most abundant in the wastewater, with a cumulative relative abundance of 78.9%. *Bacteroidota* became highly enriched in all analyzed biofilms ( $16.0 \pm 12.0$  and  $15.0 \pm 4.4\%$  for the pilot- and the bench-scale systems, respectively), while representing a relatively minor fraction of the wastewater microbiome (0.9%). The presence of ASVs affiliated to the taxa known to be strictly anaerobic (e.g., *Holophaga* spp. and *Clostridium* spp. constituting  $0.36 \pm 0.21$  and  $0.73 \pm 0.42\%$ , respectively, of the pilot plant biofilms), supported the presence of anoxic niches in the biofilms crucial for N<sub>2</sub>O reduction.

The only taxonomic group that exhibited substantial temporal variation in its relative abundance was the *Firmicutes* phylum. The relative abundances of the genera *Trichococcus*, *Lactococcus*, and *Clostridium*, affiliated to this phylum, were substantially less abundant in the pilot-plant samples collected prior to day 165 (Table S2). Low abundances of *Firmicutes* were also observed in the bench-scale reactor biofilms sampled in July and August, when the bench-scale reactor had been fed air containing 100 ppmv N<sub>2</sub>O for 6 months. Thus, it is unlikely that the increase *Firmicutes* population after day 165 was related to N<sub>2</sub>O augmentation. Rather, a more plausible rationale is that the high reactor temperatures adversely affected the *Firmicutes* population during the summer months. Also noteworthy was the distinct divergence of the biofilm communities from those of the wastewater, despite the continued introduction of wastewater microbiota to the filters. Furthermore, only 80 out of 500 of the genus-level taxa with >0.1% abundance in at least one biofilm sample could be traced back to the wastewater microbiome (Table S4).

The metagenomic analyses of the biofilms, focusing on semi-quantitative characterization of genomic potential to reduce N<sub>2</sub>O, identified diverse *nosZ* genes that belonged to both clades of *nosZ* (Figure 3c, Table S5). The abundance ratios of *nosZ* to that of the single-copy marker gene *rpoB* ranged between 2.0 and 4.4%. The cumulative abundance of clade I *nosZ* genes was 1.1- to 16.8-fold higher than that of the clade II



*nosZ* genes in all analyzed metagenomes. The *nosZ* clusters represented by *Alicyclophilus denitrificans* (clade I), *Rhodobacter* sp. C06 (clade I), *Hyphomicrobium* sp. GJ21 (clade I), a *Burkholderiales* bacterium (clade I), *Methylocella tundrae* (clade I), and *Dechloromonas* sp. H13 (clade II) were found in all four biofilms. The *Hyphomicrobium* sp. GJ21 cluster was the most abundant one among those belonging to clade I *nosZ* ( $6.5 \pm 1.3 \times 10^{-3}$  per *rpoB*), while the *Dechloromonas* sp. H13 cluster and the *Ferruginibacter* sp. BO-59 cluster were the two most abundant clade II *nosZ* clusters ( $1.7 \pm 1.6 \times 10^{-3}$  and  $3.1 \pm 3.1 \times 10^{-3}$  per *rpoB*, respectively). None of the *nosZ* genes affiliated to the *Firmicutes* phylum was found in the metagenomes, suggesting against a potential relevance of this taxon, featuring the most conspicuous temporal fluctuation in relative abundance, to the N<sub>2</sub>O-removal performance (day 165).

## DISCUSSION

Several end-of-pipe technologies for abatement of N<sub>2</sub>O emission from BNR systems have been proposed to date.<sup>18–20,45,46</sup> Yet, the technical feasibility of these technologies has been experimentally verified only in tightly controlled laboratory settings, and the environmental adversities the systems may encounter in situ have never been accounted for. The hereby studied N<sub>2</sub>O biotrickling filtration system exhibited a remarkable performance stability despite the variability in influent N<sub>2</sub>O concentrations and chemical characteristics of wastewater fed as the trickling medium. Even though the N<sub>2</sub>O concentration of the gas stream into the pilot-scale reactor remained below 20 ppmv for over 78 days after the startup, the pilot plant exhibited an immediate response to abrupt peaks in N<sub>2</sub>O concentrations between day 85 and 91 (Figure 1a). Additionally, the bench-scale reactor experiments showed that recovery of N<sub>2</sub>O removal following short-term N<sub>2</sub>O starvation was immediate. Consistently, the correlation analyses statistically corroborated the reactor system's resilience to marked variations in influent wastewater characteristics. In particular, the parameter that was expected to be the most critical was the DOC concentration, as heterotrophic O<sub>2</sub>- and N<sub>2</sub>O-respiring organisms depend on the wastewater DOC as the sole source of carbon and electrons. However, despite DOC values fluctuating between 15.6 and 40.5 mg/L, the performance of the pilot-scale reactor was unaffected. Moreover, as the influent DOC level at Gapyeong WWTP was on the low end, labile organic carbon availability is unlikely to be a factor that would limit the performance of N<sub>2</sub>O biotrickling filtration systems under realistic settings.<sup>8,47,48</sup>

The observed process stability was supported by the examination of the biofilm microbial communities. The only noticeable dynamic of the biofilm microbial communities was the modest transition from summer to fall months. The community shifts were primarily limited to ASVs affiliated to the *Firmicutes* phylum, while all pilot- and bench-scale biofilm communities were highly similar. This consistency, observed in spite of continuous ingress of the wastewater microbiota, highlights the resilience and robustness of the biofilm microbial communities, a critical feature for long-term operation of environmental bioreactors.<sup>49,50</sup> At the functional gene level, the sustained abundance of diverse *nosZ* genes in the biofilms suggested that N<sub>2</sub>O-respiring potential persisted in the biofilms regardless of the highly variable operating conditions. In both the pilot- and bench-scale reactors, the *nosZ*-to-*rpoB* ratios before and during N<sub>2</sub>O concentration alterations remained

relatively constant. As most of the abundant *nosZ* belong to facultative anaerobes, the metagenomic data are not sufficient to specifically point out the organisms responsible for actual N<sub>2</sub>O reduction.<sup>51–53</sup> Nevertheless, most of the *nosZ* genes found in high relative abundance across all biofilms belonged to the organisms with experimentally verified capability to utilize N<sub>2</sub>O as the sole electron acceptor.<sup>26,54,55</sup> Along with the consistent net *nosZ* abundance, the consistent abundance of N<sub>2</sub>O-respiring taxa, especially those affiliated or closely related to the genus *Dechloromonas* with high affinity to N<sub>2</sub>O, strongly suggests that an N<sub>2</sub>O-repairing potential can be sustained despite inconsistent N<sub>2</sub>O availability.<sup>26–28</sup>

A common dilemma for biological environmental processes has been their vulnerability to low temperatures.<sup>56–58</sup> The pilot plant operation demonstrated its resilience to moderate temperature changes while also showcasing the necessity for design considerations for an improved winter performance. Low-temperature performance is especially important for wintertime operation, as heating would incur CO<sub>2</sub> emissions that may outweigh N<sub>2</sub>O removal achieved by the system. Considering the general effect of temperature on the kinetics of microbial metabolism, the sustenance of the N<sub>2</sub>O removal activity into November, when the average daily air temperature dropped to ~5 °C, was remarkable. However, the correlation analyses showed that the reactor performance was significantly affected by the decreasing air temperature (Figure 1c). As the water temperature of the activated sludge tank was higher than 15 °C even during the coldest winter months, water-jacketing of the filter columns with wastewater as a warming agent could be a design consideration to constantly sustain the reactor temperature above 15 °C, the temperature at which the pilot-scale reactor exhibited consistent RE at ~40% (Figure 1b). Moreover, many new activated sludge WWTPs are being constructed underground for aesthetic and/or wintertime performance reasons.<sup>59–61</sup> If incorporated into the designs of these underground WWTPs, the biotrickling filtration system will not be exposed to outdoor temperatures. In sum, the vulnerability to near- or below-freezing wintry air temperatures that would diminish the applicability of the N<sub>2</sub>O biotrickling filtration system can be avoided via practical design modifications in most conceivable settings.

Beyond the proved in situ robustness of N<sub>2</sub>O biotrickling filtration under highly variable operational conditions including short-term N<sub>2</sub>O starvations, the practical and economic viability of the proposed system remains to be explored. No regulation for N<sub>2</sub>O emission is in place as of October 2022. Nor is it expected that new regulations will be promulgated in the foreseeable future, even in the most environmentally progressive regions. In this perspective, any N<sub>2</sub>O removal technologies for WWTPs need to be discussed in the context of carbon trading and, thus, the volumetric removal would be the key metric. The total amount of N<sub>2</sub>O removed during 165 days of operation without N<sub>2</sub>O augmentation, estimated via integration of EC values, amounted to 1.45 kg N<sub>2</sub>O, or 0.45 tons CO<sub>2eq</sub>. Even applying the most optimistic forecast for carbon credit price (currently traded at 74 euros per ton CO<sub>2eq</sub> as of 11/22/2022 according to <http://tradingeconomics.com>), the pilot data collected at Gapyeong WWTP would suggest against the economic viability of the technology. However, based on the multiple studies that have reported reliable long-term N<sub>2</sub>O emissions data, it can be clearly inferred that N<sub>2</sub>O concentrations or fluxes measured at full-scale BNR WWTPs are often an order of magnitude higher than those observed at

Gapyoung WWTP.<sup>8,11,12,59</sup> Considering the highest EC performance observed during the N<sub>2</sub>O augmentation period between day 203 and 207 (0.047 kg N<sub>2</sub>O in 103 h), a hypothetical application of the identical system to BNR WWTPs with an annual off-gas average N<sub>2</sub>O concentration of ~50 ppmv would be able to achieve a volumetric N<sub>2</sub>O removal as high as several tons of CO<sub>2eq</sub> yr<sup>-1</sup>. These numbers warrant a more detailed cost-to-benefit analyses with the increasing carbon price and cost reduction of further scaling, which would reduce the per-unit-volume cost. Moreover, the N<sub>2</sub>O removal system may also be adopted as a complement to PN (partial nitrification)-anammox systems widely implemented for sidestream treatment of NH<sub>4</sub><sup>+</sup>-rich anaerobic digester effluents, where N<sub>2</sub>O emissions are known to consistently occur at much higher concentrations (up to 500 ppmv; Figure S7) on a more consistent basis.<sup>62–64</sup> In this configuration, the temperature impacts would be negligible, as sidestream PN-anammox reactors are generally controlled between 30 and 35 °C.<sup>63</sup> As such, this new technology has a great potential to serve as a crucial next step toward carbon neutrality in the wastewater treatment sector, and the increasing availability of WWTP N<sub>2</sub>O emissions data will help guide the selection of the target systems where the proposed self-sustaining biotrickling filtration system would be most effective.

## ■ ASSOCIATED CONTENT

### SI Supporting Information

The Supporting Information is available free of charge at <https://pubs.acs.org/doi/10.1021/acs.est.2c08818>.

Study site information; schematic depiction of bench- and pilot-scale biotrickling filtration system; temperature comparison between ambient air and inner space of filters; N<sub>2</sub>O removal performance of pilot-, and bench-scale biotrickling filtration system; result of replicate bench-scale short-term N<sub>2</sub>O starvation test; schematic depiction of application to PN-anammox system; estimated N<sub>2</sub>O emission factors of the aerated tank; representability of representative NosZ sequences; physicochemical properties of waste water (PDF)

Genus-level microbial compositions of the wastewater and the biofilms in the pilot-scale filter (XLSX)

Genus-level microbial community compositions of the biofilms in the bench-scale filter columns (XLSX)

List of all ASVs recovered from the wastewater and the pilot-scale and bench-scale filter columns (XLSX)

Detailed phylogenetic affiliations and accession numbers (XLSX)

## ■ AUTHOR INFORMATION

### Corresponding Author

**Sukhwan Yoon** – Department of Civil and Environmental Engineering, Korea Advanced Institute of Science and Technology (KAIST), Daejeon 34141, South Korea; [orcid.org/0000-0002-9933-7054](https://orcid.org/0000-0002-9933-7054); Phone: +82 10-3461-2024; Email: [syoon80@kaist.ac.kr](mailto:syoon80@kaist.ac.kr); Fax: +82 42-350-3610

### Authors

**Heejoon Han** – Department of Civil and Environmental Engineering, Korea Advanced Institute of Science and Technology (KAIST), Daejeon 34141, South Korea

**Daehyun D. Kim** – Department of Civil and Environmental Engineering, Korea Advanced Institute of Science and

Technology (KAIST), Daejeon 34141, South Korea;

[orcid.org/0000-0002-7234-4721](https://orcid.org/0000-0002-7234-4721)

**Min Joon Song** – Department of Civil and Environmental Engineering, Korea Advanced Institute of Science and Technology (KAIST), Daejeon 34141, South Korea

**Taeho Yun** – Department of Civil and Environmental Engineering, Korea Advanced Institute of Science and Technology (KAIST), Daejeon 34141, South Korea

**Hyun Yoon** – Department of Civil and Environmental Engineering, Korea Advanced Institute of Science and Technology (KAIST), Daejeon 34141, South Korea; School of Civil & Environmental Engineering, Cornell University, Ithaca, New York 14853, United States

**Hong Woon Lee** – Daega Powder Systems Co., Seoul 08262, South Korea

**Young Mo Kim** – Department of Civil and Environmental Engineering, Hanyang University, Seoul 04763, South Korea

**Michele Laurenzi** – Department of Geoscience and Engineering, Delft University of Technology, 2628 CN Delft, The Netherlands

Complete contact information is available at:

<https://pubs.acs.org/10.1021/acs.est.2c08818>

## Notes

The authors declare no competing financial interest.

## ■ ACKNOWLEDGMENTS

This work was supported by the “R&D Center for reduction of non-CO<sub>2</sub> greenhouse gases (2017002420002)” funded by the Korea Ministry of Environment. The authors H.H. and S.Y. were also supported by the National Research Foundation of Korea (2020R1C1C100797013) and the Ministry of Environment (NIBR202221204), and M.L. was supported by a VENI grant from the Dutch Research Council NWO (VI.Veni.192.252).

## ■ REFERENCES

- (1) Rahman, S. M.; Eckelman, M. J.; Onnis-Hayden, A.; Gu, A. Z. Life-cycle assessment of advanced nutrient removal technologies for wastewater treatment. *Environ. Sci. Technol.* **2016**, *50*, 3020–3030.
- (2) McCarty, P. L. What is the best biological process for nitrogen removal: when and why? *Environ. Sci. Technol.* **2018**, *52*, 3835–3841.
- (3) Kampschreur, M. J.; Temmink, H.; Kleerebezem, R.; Jetten, M. S.; van Loosdrecht, M. C. M. Nitrous oxide emission during wastewater treatment. *Water Res.* **2009**, *43*, 4093–4103.
- (4) Kuypers, M. M.; Marchant, H. K.; Kartal, B. The microbial nitrogen-cycling network. *Nat. Rev. Microbiol.* **2018**, *16*, 263–276.
- (5) Wuebbles, D. J. Nitrous oxide: no laughing matter. *Science* **2009**, *326*, 56–57.
- (6) Law, Y.; Ye, L.; Pan, Y.; Yuan, Z. Nitrous oxide emissions from wastewater treatment processes. *Philos. Trans. R. Soc., B* **2012**, *367*, 1265–1277.
- (7) Pachauri, R. K.; Allen, M. R.; Barros, V. R.; Broome, J.; Cramer, W.; Christ, R.; Church, J. A.; Clarke, L.; Dahe, Q.; Dasgupta, P. *Climate Change 2014: Synthesis Report. Contribution of Working Groups I, II and III to the Fifth Assessment Report of the Intergovernmental Panel on Climate Change*; IPCC: Geneva, Switzerland, 2014.
- (8) Song, M. J.; Choi, S.; Bae, W. B.; Lee, J.; Han, H.; Kim, D. D.; Kwon, M.; Myung, J.; Kim, Y. M.; Yoon, S. Identification of primary effectors of N<sub>2</sub>O emissions from full-scale biological nitrogen removal systems using random forest approach. *Water Res.* **2020**, *184*, 116144.
- (9) Wunderlin, P.; Mohn, J.; Joss, A.; Emmenegger, L.; Siegrist, H. Mechanisms of N<sub>2</sub>O production in biological wastewater treatment under nitrifying and denitrifying conditions. *Water Res.* **2012**, *46*, 1027–1037.



- (10) Ahn, J. H.; Kim, S.; Park, H.; Rahm, B.; Pagilla, K.; Chandran, K. N<sub>2</sub>O emissions from activated sludge processes, 2008–2009: results of a national monitoring survey in the United States. *Environ. Sci. Technol.* **2010**, *44*, 4505–4511.
- (11) Valk, L. C.; Peces, M.; Singleton, C. M.; Laursen, M. D.; Andersen, M. H.; Mielczarek, A. T.; Nielsen, P. H. Exploring the microbial influence on seasonal nitrous oxide concentration in a full-scale wastewater treatment plant using metagenome assembled genomes. *Water Res.* **2022**, *219*, 118563.
- (12) Gruber, W.; von Känel, L.; Vogt, L.; Luck, M.; Biolley, L.; Feller, K.; Moosmann, A.; Krähnenbühl, N.; Kipf, M.; Loosli, R.; Vogel, M.; Morgenroth, E.; Braun, D.; Joss, A. Estimation of countrywide N<sub>2</sub>O emissions from wastewater treatment in Switzerland using long-term monitoring data. *Water Res.: X* **2021**, *13*, 100122.
- (13) Duan, H.; Zhao, Y.; Koch, K.; Wells, G. F.; Zheng, M.; Yuan, Z.; Ye, L. Insights into nitrous oxide mitigation strategies in wastewater treatment and challenges for wider implementation. *Environ. Sci. Technol.* **2021**, *55*, 7208–7224.
- (14) Itokawa, H.; Hanaki, K.; Matsuo, T. Nitrous oxide production in high-loading biological nitrogen removal process under low COD/N ratio condition. *Water Res.* **2001**, *35*, 657–664.
- (15) Talleg, G.; Garnier, J.; Billen, G.; Gousailles, M. Nitrous oxide emissions from secondary activated sludge in nitrifying conditions of urban wastewater treatment plants: effect of oxygenation level. *Water Res.* **2006**, *40*, 2972–2980.
- (16) Duan, H.; van den Akker, B.; Thwaites, B. J.; Peng, L.; Herman, C.; Pan, Y.; Ni, B.-J.; Watt, S.; Yuan, Z.; Ye, L. Mitigating nitrous oxide emissions at a full-scale wastewater treatment plant. *Water Res.* **2020**, *185*, 116196.
- (17) Chen, X.; Mielczarek, A. T.; Habicht, K.; Andersen, M. H.; Thornberg, D.; Sin, G. Assessment of Full-Scale N<sub>2</sub>O Emission characteristics and testing of control concepts in an activated sludge wastewater treatment plant with alternating aerobic and anoxic phases. *Environ. Sci. Technol.* **2019**, *53*, 12485–12494.
- (18) Frutos, O. D.; Quijano, G.; Pérez, R.; Muñoz, R. Simultaneous biological nitrous oxide abatement and wastewater treatment in a denitrifying off-gas bioscrubber. *Chem. Eng. J.* **2016**, *288*, 28–37.
- (19) Yoon, H.; Song, M. J.; Yoon, S. Design and feasibility analysis of a self-sustaining biofiltration system for removal of low concentration N<sub>2</sub>O emitted from wastewater treatment plants. *Environ. Sci. Technol.* **2017**, *51*, 10736–10745.
- (20) Yoon, H.; Song, M. J.; Kim, D. D.; Sabba, F.; Yoon, S. A serial biofiltration system for effective removal of low-concentration nitrous oxide in oxic gas streams: mathematical modeling of reactor performance and experimental validation. *Environ. Sci. Technol.* **2019**, *53*, 2063–2074.
- (21) Ritalahti, K. M.; Löffler, F. E.; Rasch, E. E.; Koenigsberg, S. S. Bioaugmentation for chlorinated ethene detoxification: Bioaugmentation and molecular diagnostics in the bioremediation of chlorinated ethene-contaminated sites. *Ind. Biotechnol.* **2005**, *1*, 114–118.
- (22) Williams, K. H.; Bargar, J. R.; Lloyd, J. R.; Lovley, D. R. Bioremediation of uranium-contaminated groundwater: a systems approach to subsurface biogeochemistry. *Curr. Opin. Biotechnol.* **2013**, *24*, 489–497.
- (23) Salanitro, J. P.; Johnson, P. C.; Spinnler, G. E.; Maner, P. M.; Wisniewski, H. L.; Bruce, C. Field-scale demonstration of enhanced MTBE bioremediation through aquifer bioaugmentation and oxygenation. *Environ. Sci. Technol.* **2000**, *34*, 4152–4162.
- (24) Shan, J.; Sanford, R. A.; Chee-Sanford, J.; Ooi, S. K.; Löffler, F. E.; Konstantinidis, K. T.; Yang, W. H. Beyond denitrification: the role of microbial diversity in controlling nitrous oxide reduction and soil nitrous oxide emissions. *Global Change Biol.* **2021**, *27*, 2669–2683.
- (25) Shu, X.; Daniell, T. J.; Hallett, P. D.; Baggs, E. M.; Mitchell, S.; Langarica-Fuentes, A.; Griffiths, B. S. Role of microbial communities in conferring resistance and resilience of soil carbon and nitrogen cycling following contrasting stresses. *Eur. J. Soil Biol.* **2021**, *104*, 103308.
- (26) Yoon, S.; Nissen, S.; Park, D.; Sanford, R. A.; Löffler, F. E. Nitrous oxide reduction kinetics distinguish bacteria harboring clade I versus clade II nosZ. *Appl. Environ. Microbiol.* **2016**, *82*, 3793–3800.
- (27) Suenaga, T.; Hori, T.; Riya, S.; Hosomi, M.; Smets, B. F.; Terada, A. Enrichment, isolation, and characterization of high-affinity N<sub>2</sub>O-reducing bacteria in a gas-permeable membrane reactor. *Environ. Sci. Technol.* **2019**, *53*, 12101–12112.
- (28) Qi, C.; Zhou, Y.; Suenaga, T.; Oba, K.; Lu, J.; Wang, G.; Zhang, L.; Yoon, S.; Terada, A. Organic carbon determines nitrous oxide consumption activity of clade I and II nosZ bacteria: genomic and biokinetic insights. *Water Res.* **2022**, *209*, 117910.
- (29) Kim, D. D.; Park, D.; Yoon, H.; Yun, T.; Song, M. J.; Yoon, S. Quantification of nosZ genes and transcripts in activated sludge microbiomes with novel group-specific qPCR methods validated with metagenomic analyses. *Water Res.* **2020**, *185*, 116261.
- (30) Nierychlo, M.; Andersen, K. S.; Xu, Y.; Green, N.; Jiang, C.; Albertsen, M.; Dueholm, M. S.; Nielsen, P. H. MiDAS 3: an ecosystem-specific reference database, taxonomy and knowledge platform for activated sludge and anaerobic digesters reveals species-level microbiome composition of activated sludge. *Water Res.* **2020**, *182*, 115955.
- (31) Lu, H.; Chandran, K. Factors promoting emissions of nitrous oxide and nitric oxide from denitrifying sequencing batch reactors operated with methanol and ethanol as electron donors. *Biotechnol. Bioeng.* **2010**, *106*, 390–398.
- (32) Suenaga, T.; Riya, S.; Hosomi, M.; Terada, A. Biokinetic characterization and activities of N<sub>2</sub>O-reducing bacteria in response to various oxygen levels. *Front. Microbiol.* **2018**, *9*, 697.
- (33) Desloover, J.; Roobroeck, D.; Heylen, K.; Puig, S.; Boeckx, P.; Verstraete, W.; Boon, N. Pathway of nitrous oxide consumption in isolated *Pseudomonas stutzeri* strains under anoxic and oxic conditions. *Environ. Microbiol.* **2014**, *16*, 3143–3152.
- (34) Miranda, K. M.; Espey, M. G.; Wink, D. A. A rapid, simple spectrophotometric method for simultaneous detection of nitrate and nitrite. *Nitric Oxide* **2001**, *5*, 62–71.
- (35) Hood-Nowotny, R.; Umana, N. H.-N.; Inselbacher, E.; Oswald-Lachouani, P.; Wanek, W. Alternative methods for measuring inorganic, organic, and total dissolved nitrogen in soil. *Soil Sci. Soc. Am. J.* **2010**, *74*, 1018–1027.
- (36) Bolyen, E.; Rideout, J. R.; Dillon, M. R.; Bokulich, N. A.; Abnet, C. C.; Al-Ghalith, G. A.; Alexander, H.; Alm, E. J.; Arumugam, M.; Asnicar, F.; Bai, Y.; Bisanz, J. E.; Bittinger, K.; Brejnrod, A.; Brislawn, C. J.; Brown, C. T.; Callahan, B. J.; Caraballo-Rodríguez, A. M.; Chase, J.; Cope, E. K.; Da Silva, R.; Diener, C.; Dorrestein, P. C.; Douglas, G. M.; Durall, D. M.; Duvallet, C.; Edwardson, C. F.; Ernst, M.; Estaki, M.; Fouquier, J.; Gauglitz, J. M.; Gibbons, S. M.; Gibson, D. L.; Gonzalez, A.; Gorlick, K.; Guo, J.; Hillmann, B.; Holmes, S.; Holste, H.; Huttenhower, C.; Huttley, G. A.; Janssen, S.; Jarmusch, A. K.; Jiang, L.; Kaehler, B. D.; Kang, K. B.; Keefe, C. R.; Keim, P.; Kelley, S. T.; Knights, D.; Koester, I.; Kosciulek, T.; Kreps, J.; Langille, M. G. I.; Lee, J.; Ley, R.; Liu, Y.-X.; Loftfield, E.; Lozupone, C.; Maher, M.; Marotz, C.; Martin, B. D.; McDonald, D.; McIver, L. J.; Melnik, A. V.; Metcalf, J. L.; Morgan, S. C.; Morton, J. T.; Naimey, A. T.; Navas-Molina, J. A.; Nothias, L. F.; Orchanian, S. B.; Pearson, T.; Peoples, S. L.; Petras, D.; Preuss, M. L.; Pruesse, E.; Rasmussen, L. B.; Rivers, A.; Robeson, M. S.; Rosenthal, P.; Segata, N.; Shaffer, M.; Shiffer, A.; Sinha, R.; Song, S. J.; Spear, J. R.; Swafford, A. D.; Thompson, L. R.; Torres, P. J.; Trinh, P.; Tripathi, A.; Turnbaugh, P. J.; Ul-Hasan, S.; van der Hooft, J. J. J.; Vargas, F.; Vázquez-Baeza, Y.; Vogtmann, E.; von Hippel, M.; Walters, W.; Wan, Y.; Wang, M.; Warren, J.; Weber, K. C.; Williamson, C. H. D.; Willis, A. D.; Xu, Z. Z.; Zaneveld, J. R.; Zhang, Y.; Zhu, Q.; Knight, R.; Caporaso, J. G. Reproducible, interactive, scalable and extensible microbiome data science using QIIME 2. *Nat. Biotechnol.* **2019**, *37*, 852–857.
- (37) Nurk, S.; Meleshko, D.; Korobeynikov, A.; Pevzner, P. A. metaSPAdes: a new versatile metagenomic assembler. *Genome Res.* **2017**, *27*, 824–834.

- (38) Hyatt, D.; Chen, G. L.; LoCascio, P. F.; Land, M. L.; Larimer, F. W.; Hauser, L. J. Prodigal: prokaryotic gene recognition and translation initiation site identification. *BMC Bioinf.* **2010**, *11*, 119.
- (39) Buchfink, B.; Xie, C.; Huson, D. H. Fast and sensitive protein alignment using DIAMOND. *Nat. Methods* **2015**, *12*, 59–60.
- (40) Langmead, B.; Salzberg, S. L. Fast gapped-read alignment with Bowtie 2. *Nat. Methods* **2012**, *9*, 357–359.
- (41) Li, H.; Handsaker, B.; Wysoker, A.; Fennell, T.; Ruan, J.; Homer, N.; Marth, G.; Abecasis, G.; Durbin, R. The sequence alignment/map format and SAMtools. *Bioinformatics* **2009**, *25*, 2078–2079.
- (42) Case, R. J.; Boucher, Y.; Dahllöf, I.; Holmström, C.; Doolittle, W. F.; Kjelleberg, S. Use of 16S rRNA and rpoB genes as molecular markers for microbial ecology studies. *Appl. Environ. Microbiol.* **2007**, *73*, 278–288.
- (43) Li, W.; Godzik, A. Cd-hit: a fast program for clustering and comparing large sets of protein or nucleotide sequences. *Bioinformatics* **2006**, *22*, 1658–1659.
- (44) RStudio Team. *RStudio: Integrated Development for R*; RStudio, Inc.: Boston, MA, 2020.
- (45) Frutos, O. D.; Quijano, G.; Aizpuru, A.; Muñoz, R. A state-of-the-art review on nitrous oxide control from waste treatment and industrial sources. *Biotechnol. Adv.* **2018**, *36*, 1025–1037.
- (46) Frutos, O. D.; Cortes, I.; Cantera, S.; Arnaiz, E.; Lebrero, R.; Muñoz, R. Nitrous oxide abatement coupled with biopolymer production as a model GHG biorefinery for cost-effective climate change mitigation. *Environ. Sci. Technol.* **2017**, *51*, 6319–6325.
- (47) Escalas, A.; Droguet, M.; Guadayol, J. M.; Caixach, J. Estimating DOC regime in a wastewater treatment plant by UV deconvolution. *Water Res.* **2003**, *37*, 2627–2635.
- (48) Katsoyiannis, A.; Samara, C. The fate of dissolved organic carbon (DOC) in the wastewater treatment process and its importance in the removal of wastewater contaminants. *Environ. Sci. Pollut. Res. Int.* **2007**, *14*, 284–292.
- (49) Navada, S.; Knutsen, M. F.; Bakke, I.; Vadstein, O. Nitrifying biofilms deprived of organic carbon show higher functional resilience to increases in carbon supply. *Sci. Rep.* **2020**, *10*, 7121.
- (50) Weissbrodt, D. G.; Shani, N.; Holliger, C. Linking bacterial population dynamics and nutrient removal in the granular sludge biofilm ecosystem engineered for wastewater treatment. *FEMS Microbiol. Ecol.* **2014**, *88*, 579–595.
- (51) Jones, C. M.; Graf, D. R.; Bru, D.; Philippot, L.; Hallin, S. The unaccounted yet abundant nitrous oxide-reducing microbial community: A potential nitrous oxide sink. *ISME J.* **2013**, *7*, 417–426.
- (52) Park, D.; Kim, H.; Yoon, S. Nitrous oxide reduction by an obligate aerobic bacterium, *Gemmatimonas aurantiaca* strain T-27. *Appl. Environ. Microbiol.* **2017**, *83*, e00502–e00517.
- (53) Sanford, R. A.; Wagner, D. D.; Wu, Q.; Chee-Sanford, J. C.; Thomas, S. H.; Cruz-García, C.; Rodríguez, G.; Massol-Deyá, A.; Krishnani, K. K.; Ritalahti, K. M.; Nissen, S.; Konstantinidis, K. T.; Löffler, F. E. Unexpected nondenitrifier nitrous oxide reductase gene diversity and abundance in soils. *Proc. Natl. Acad. Sci.* **2012**, *109*, 19709–19714.
- (54) Klueglein, N.; Kappler, A. Abiotic oxidation of Fe(II) by reactive nitrogen species in cultures of the nitrate-reducing Fe(II) oxidizer *Acidovorax* sp. BoFeN1 – questioning the existence of enzymatic Fe(II) oxidation. *Geobiology* **2013**, *11*, 180–190.
- (55) Martineau, C.; Mauffrey, F.; Villemur, R. Comparative analysis of denitrifying activities of *Hyphomicrobium nitratorans*, *Hyphomicrobium denitrificans*, and *Hyphomicrobium zavarzinii*. *Appl. Environ. Microbiol.* **2015**, *81*, S003–S014.
- (56) Cao, Y.; van Loosdrecht, M. C. M.; Daigger, G. T. Mainstream partial nitrification–anammox in municipal wastewater treatment: status, bottlenecks, and further studies. *Appl. Microbiol. Biotechnol.* **2017**, *101*, 1365–1383.
- (57) Moll, D. M.; Summers, R. S.; Fonseca, A. C.; Matheis, W. Impact of temperature on drinking water biofilter performance and microbial community structure. *Environ. Sci. Technol.* **1999**, *33*, 2377–2382.
- (58) Randall, C. W.; Barnard, J. L.; Stensel, H. D. *Design and Retrofit of Wastewater Treatment Plants for Biological Nutrient Removal*, 5th ed.; CRC Press, 1998.
- (59) Kosonen, H.; Heinonen, M.; Mikola, A.; Haimi, H.; Mulas, M.; Corona, F.; Vahala, R. Nitrous oxide production at a fully covered wastewater treatment plant: results of a long-term online monitoring campaign. *Environ. Sci. Technol.* **2016**, *50*, 5547–5554.
- (60) Baresel, C.; Andersson, S.; Yang, J.; Andersen, M. H. Comparison of nitrous oxide (N<sub>2</sub>O) emissions calculations at a Swedish wastewater treatment plant based on water concentrations versus off-gas concentrations. *Adv. Clim. Change Res.* **2016**, *7*, 185–191.
- (61) Broere, W. Urban underground space: Solving the problems of today's cities. *Tunn. Undergr. Space Technol.* **2016**, *55*, 245–248.
- (62) Castro-Barros, C. M.; Daelman, M.; Mampaey, K.; van Loosdrecht, M. C. M.; Volcke, E. Effect of aeration regime on N<sub>2</sub>O emission from partial nitrification-anammox in a full-scale granular sludge reactor. *Water Res.* **2015**, *68*, 793–803.
- (63) Mampaey, K. E.; De Kreuk, M. K.; van Dongen, U. G.; van Loosdrecht, M. C. M.; Volcke, E. I. Identifying N<sub>2</sub>O formation and emissions from a full-scale partial nitrification reactor. *Water Res.* **2016**, *88*, 575–585.
- (64) Fenu, A.; Smolders, S.; De Gussem, K.; Weemaes, M. Conflicting carbon footprint and energy saving in a side-stream anammox process. *Biochem. Eng. J.* **2019**, *151*, 107336.

## Recommended by ACS

### Biological Filtration is Resilient to Wildfire Ash-Associated Organic Carbon Threats to Drinking Water Treatment

Emma A. J. Blackburn, Monica B. Emelko, *et al.*

FEBRUARY 24, 2023

ACS ES&T WATER

READ 

### Environmental and Economic Impacts of Managing Nutrients in Digestate Derived from Sewage Sludge and High-Strength Organic Waste

Kevin D. Orner, Arpad Horvath, *et al.*

NOVEMBER 21, 2022

ENVIRONMENTAL SCIENCE & TECHNOLOGY

READ 

### Elimination of Complex Process Control Strategies in Single-Stage Deammonification

Carolyn L. Coffey, Linda A. Figueroa, *et al.*

JULY 13, 2021

ACS ES&T ENGINEERING

READ 

### Widespread but Overlooked DNRA Process in a Full-Scale Simultaneous Partial Nitrification, Anammox, and Denitrification Plant

Zhibin Wang, Shou-Qing Ni, *et al.*

JUNE 30, 2022

ACS ES&T WATER

READ 

Get More Suggestions >